International Journal of Latest Engineering and Management Research (IJLEMR)
ISSN: 2455-4847
www.ijlemr.com || Volume 04 - Issue 03 || March 2019 || PP. 90-96

Synthesis, Characterization and Antimicrobial Applications of AI Gum Stabilized Cobalt Doped ZnO Nanoparticles

Dr. R. Sakthivel[1], A. Geetha[2], Ba. Anandh[3], A. Shankar Ganesh[4]
[1,3,4] Associate Professor , [1]Dept of Electronics,
[2]Ph.D Research Scholar, Dept of Chemistry,
PSG College of Arts & Science, Coimbatore

Abstract: The AI gum stabilized Cobalt doped ZnO nanoparticles were synthesized by the wet chemical method. The structural, morphology properties, antibacterial and antifungal activities were studied for AI stabilised different cobalt concentration. X-Ray Diffraction (XRD) pattern confirms the crystalline nature and it exhibits hexagonal structure along with c-axis orientation. Field Emission Scanning Electron Microscope (FESEM) confirms the occurrence of a spherical shaped structure. Energy Dispersive X-ray (EDAX) results confirms the existence of zinc, cobalt and oxygen atoms.. Antibacterial activities against S.aureus (Gram-positive) show the maximum zone of inhibition when compared to E. coli (Gram-negative). Antifungal activities against Aspergillussp show the maximum zone of inhibition when compared to Candida albican were also studied.

Keywords: Antibacterial and antifungal activity, EDAX, FESEM, XRD, ZnO

I. Introduction

ZnO is a direct wide band gap (3.2 eV at room temperature) II–IV group semiconductor which has been used in many applications. ZnO is preferred due to its abundance, low cost, and environmentally friendly nature. ZnO can be used for diodes [1], optoelectronics [2], biosensors [3] gas sensors [4], transparent conductive oxide [5], anti-bacterial agents [6] .Nowadays, efforts have been made to improve the properties of ZnO nanostructures by doping various chemical elements such as Ga [7, 8], In [9, 10], Sn [11], Mn [12], Mg [13], Bi [14] and Al [15, 16] into ZnO structures. Among the above mentioned dopants, Cobalt have suited well for tailoring the electronic structure. The substitution Co^{2+} at the Zn^{2+} tetrahedrally ligand-coordinated (T_d) sites in the ZnO host lattice give rise to strong absorption peaks in the visible range, due to transitions between Co 3d ligand field split states and fully occupied 3d electron shell of Zn^{2+}[17]. These transitions induce photoconductivity of the Cobalt doped ZnO nanoparticles and enhance the photocatalytic activity [18]. Hence, we have selected cobalt (Co) doping into ZnO in order to increase the photocatalytic and antimicrobial properties. This paper deals with the structural and antimicrobial properties of AI stabilised Co doped ZnO nanoparticles.

II. Materials and Methods

2.1 Materials

All the reagents used in the present work were purchased from Sigma-Aldrich Germany (99.9% purity) and used without further purification. Co doped ZnO nanoparticles were prepared
using zinc nitrate, sodium hydroxide and *Azadirachta indica* gum as a stabilizing agent. Double distilled water was used as a solvent.

2.2 Synthesis of Co doped ZnO nanoparticles

The gum exudates of *Azadirachta indica* were collected from PSG college of Arts and science campus (Coimbatore, Tamil Nadu and India) and authenticated by Botanical Survey of India (BSI), Coimbatore were washed with double distilled water to remove impurities. After complete dissolution of gum, it was filtered through Whatman filter paper (no: 40) and kept in dessicator to get a glassy mass of purified gum.

High purity metal doped ZnO nanoparticles were synthesized using a simple wet chemical method. About 1 g of zinc nitrate was dissolved in 90 ml of double distilled water. After 10 minutes stirring, about 0.1 g of AI gum in 10 ml water was added. To this mixture stochiometric quantities of cobalt nitrate solution (0.03, 0.05 and 0.07) was added. This is continued by the addition of about 100 ml of NaOH solution in drop wise with vigorous stirring for 3 hours. The suspension were centrifuged and dried in hot air oven at 100^{o} C. The light green crystalline powder of Co doped ZnO nanoparticles was obtained.

2.3Antibacterial assay

The agar well diffusion method was used to screen the antibacterial activity of ZnO and AI gum stabilized ZnO nanoparticles. For these experiments, Gram-negative bacteria *Escherichia coli* and Gram-positive bacteria *Staphylococcus aureus* were employed in the study. Muller Hinton agar was prepared and sterilized. The test specimens were swabbed over the agar surface using the sterile cotton swab. Wells were made on the agar surface using sterile the gel puncture and about 10µl of the sample were loaded onto the wells and the plates were incubated at 37 C for 24 hours. The clear zones were used to determine the efficiency of the samples.

2.4 Antifungal assay

The activity of the given sample on various fungal strains was assayed by well diffusion method. The fungicidal effect of the given sample can be assessed by the inhibition of mycelia growth of the fungus and was observed as a zone of inhibition near the wells.

Aspergillus fumigates and Candida albican obtained from PSG IMSR hospital were used to assess the anti-fungal activity of the plant extracts. Potato dextrose agar was prepared and sterilized and poured on to the petriplates. In each plate different test fungal cultures were swabbed over the agar surface using the sterile cotton swab. Wells were made on the agar surface using the sterile gel puncture and about 100 µl of the given samples were loaded onto the wells. The plates were incubated at room temperature for 3 days and the antifungal effect was seen as crescent shaped zones of inhibition.

III. Results and Discussion

3.1 XRD analysis

Figure.1 shows the XRD pattern of ZnO nanoparticles for different Co concentration. The strong and clear peaks reveal the high purity and crystallinity of the samples. The sharp diffraction peaks corresponding to (100), (002), and (101) planes indicate the crystalline ZnO with hexagonal wurtzite structure, which is in close agreement with the standard card (JCPDS Card No. 36-1451).

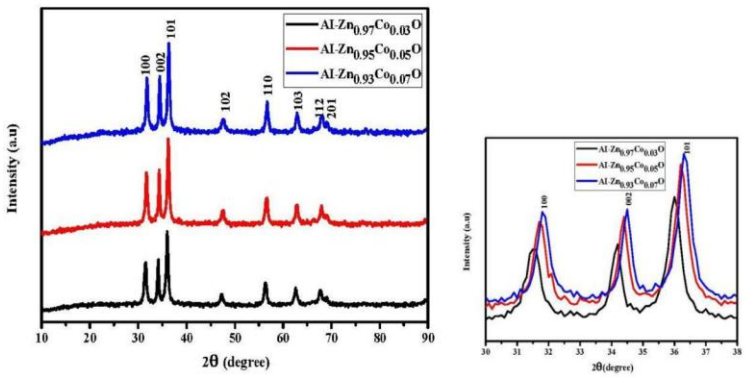

Figure 1: XRD pattern of AI gum stabilized Co doped ZnO nanoparticles

It is evident from the XRD data that no additional peaks related to cobalt metal and other oxide phases were detected which illustrates that the obtained Co doped ZnO nanoparticles are of single phase. The crystallite size (D), of the nanoparticles was estimated by the Scherrer's formula [19].

Table 1: Structural parameters of AI gum stabilized Co doped ZnO nanoparticles

S. No	Sample code	*hkl*	2θ (degree)		d (A^o)		FWHM	Crystal size D (nm)
			Observed	JCPDS	Observed	JCPDS		
1	AI-Zn0.97Co0.03O	100	31.48	31.77	2.83	2.81	0.5382	15
		002	34.13	34.42	2.62	2.60	0.5731	15
		101	35.97	36.25	2.49	2.48	0.4569	18
2	AI-Zn0.95 Co0.05O	100	31.70	31.77	2.82	2.81	0.5299	16
		002	34.34	34.42	2.60	2.60	0.5197	16
		101	36.19	36.25	2.47	2.48	0.4535	18
3	AI-Zn0.93Co0.07O	100	31.80	31.77	2.81	2.81	0.5355	16
		002	34.45	34.42	2.60	2.60	0.5148	16
		101	36.29	36.25	2.47	2.48	0.4493	19

The full width half maximum values (FWHM), 2θ values with their corresponding *hkl* values and calculated crystallite sizes are presented in Table 1. For the undoped AI-ZnO(1) the crystallite size is 15 nm. Analysis of the data shows, in cobalt doped ZnO the crystallite size increases from 16 to 18 nm with increasing the dopant concentration from 0.03 to 0.07 g. The small increase in crystal size may due to the less solubility of cobalt in the ZnO matrix. The lattice parameters 'a' and 'c' values, strain(ε) and dislocation density(δ) are given in Table 2.

Table 2: Lattice parameters of AI gum stabilized Co doped ZnO nanoparticles

S. No	Samples	Lattice parameters (A^o)		Strain ε (10^{-3})	Dislocation density δ
		A	C		
1	AI-ZnO(1)	3.268	5.233	2.461	5.0420 E+15
2	AI-Zn0.97Co0.03O	3.2798	5.2518	2.259	4.2477 E+15
3	AI-Zn0.95Co0.05O	3.2580	5.2203	2.247	4.1133 E+15
4	AI-Zn0.93Co0.07O	3.2478	5.2042	2.223	4.2007 E+15

The calculated 'a' and 'c' values of cobalt doped ZnO nanoparticles are higher than the undoped AI-ZnO(1) and the values are close to the JCPDS card values of pure hexagonal ZnO nanoparticles (a = 3.251 & c = 5.212). The increase in lattice constants may be due to the replacement of Zn^{2+} by Co^{2+} ion in the ZnO lattice. The strain and the dislocation density increases in Zn0.97Co0.03O nanoparticles and then increases for higher doping concentration (Zn0.95Co0.05O & Zn0.93Co0.07O). The change in lattice parameter value may be due to the difference in ionic radii between Co (0.78 Å) and Zn (0.74 Å) and also in wurtzite structure the Co^{2+} are present in an octahedral environment. As a consequence, the XRD peak was shifted, which is attributed to increase in reduction and lattice strain [20].

The increase in particle size confirmed the cobalt incorporation into the ZnO lattice. The substitution of Co^{2+} in an interstitial position would affect the concentration of the interstitial Zn, oxygen, and Zn vacancies. The observation of small changes of 2θ values in diffraction peaks and peak narrowing is due to the increase of microstrain, and the line broadening may be due to the increase in size (15 to 18 nm) and microstrain of nanoparticles. The structural change obtained from the diffraction peaks illustrates the incorporation of Co^{2+} ions into the ZnO lattice, which indicates that the crystal lattice has no obvious change by Co doping.

3.2 FESEM and EDX analysis

Field emission scanning electron microscopy (FESEM) was used to study the surface morphology and average particle of the Co^{2+} doped ZnO nanoparticles. Figure 3 shows FESEM images of AI gum stabilized Co doped ZnO nanoparticles with different Co concentrations.

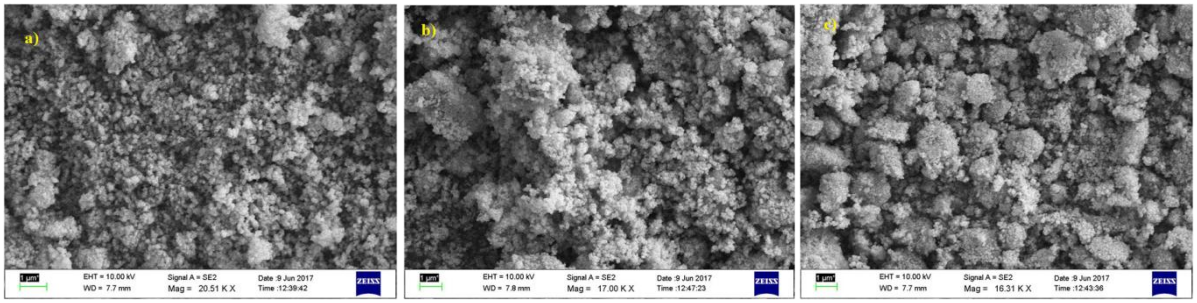

Figure 3: FESEM images of a) AI-Zn0.97Co0.03 O b) AI-Zn0.95Co0.05 O
c) AI-Zn0.93Co0.07 O nanoparticles

It was evidently seen that all the particles have spherical shape. Increasing of doping concentration of Co into ZnO undergoes self agglomeration leading to increase in particle size which is confirmed by XRD results. The extent of incorporation of Co and composition of AI gum stabilized Co doped ZnO nanoparticles were analyzed by EDX analysis

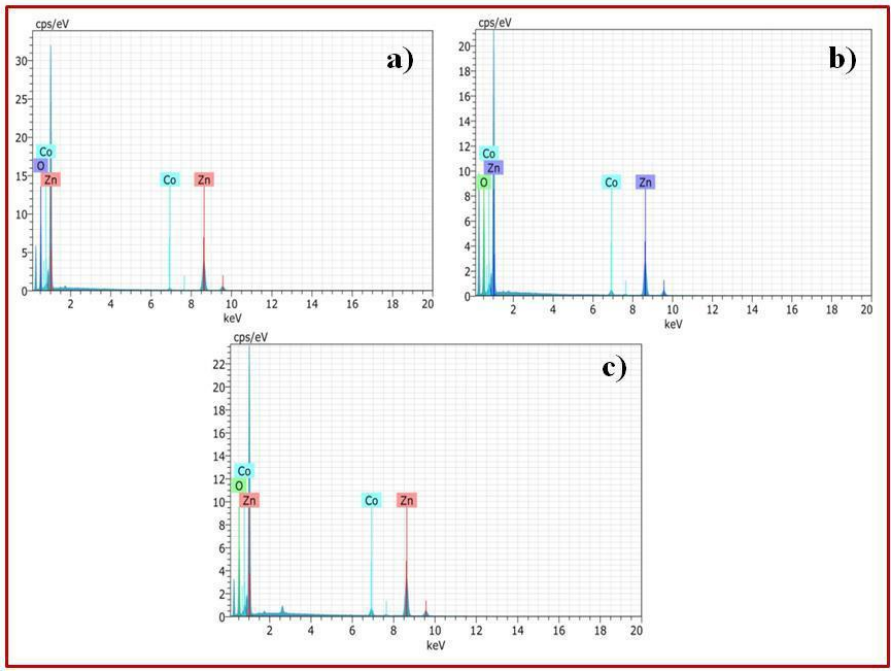

Figure 4: EDX spectra of a) AI-Zn0.97Co0.03O b) AI-Zn0.95Co0.05O
c) AI-Zn0.93Co0.07O nanoparticles

Figure 4 shows the Energy dispersive X-ray spectra ofAI gum stabilized Co doped ZnO nanoparticles with different Co concentrations. The EDX spectrum shows three peaks corresponding to the elements Co, O and Zn only indicating the insertion of Co^{2+} into the ZnO matrix. Elemental composition of Co doped ZnO nanoparticles were shown in Table .3. The atomic percentage proves the phase purity of the doped ZnO nanoparticles.

Table 3: Elemental composition of AI gum stabilized Co doped ZnO nanoparticles

S. No	Sample code	Zn (atomic %)	Co (atomic %)	Oxygen (atomic %)
1	AI-Zn0.97Co0.03O	32.21	0.78	67.01
2	AI-Zn0.95Co0.05O	29.44	1.97	68.59
3	AI-Zn0.93Co0.07O	36.53	3.04	60.43

3.3 Antibacterial applications

AI gum stabilized Co doped ZnO nanoparticles were subjected to antibacterial activity for four pathogenic (gram-negative *E.coli*, and gram positive(*S.aureus*) bacteria. Well diffusion test was carried out on Nutrient agar to observe the antibacterial activity against pathogenic organisms. The zone of inhibition of the AI gum stabilized Co doped ZnO nanoparticles are shown in Figure 5 and the values are given in Table 4. Antibacterial activity of the undoped AI-ZnO(1) is found to increase with increase in Co doping concentration. The abrasive surface texture also increases the antibacterial activity of ZnO which is obtained by doping with transition metals (Co) [21]. From the earlier reports the antibacterial activity of ZnO were explained by the formation of reactive oxygen species, release of Zn^{2+} ions and membrane dysfunction [22]. The maximum antibacterial activity was found in the AI gum stabilized 7% Co doped ZnO against *S.aureus.* Snega *et al* [23] have investigated the higher antibacterial activity for gram positive bacteria than negative bacteria the negatively charged radicals easily attach to the cell wall of gram positive bacteria thus kills the bacteria.

Table 4: Antibacterial assay of AI gum stabilized Co doped ZnO nanoparticles

S. No.	Samples	Zone of inhibition (mm)	
		Escherichia Coli	*Staphylococcus aureus*
1	AI-Zn0.97Co0.03O	11	17
2	AI-Zn0.95Co0.05O	14	20
3	AI-Zn0.93Co0.07O	22	23

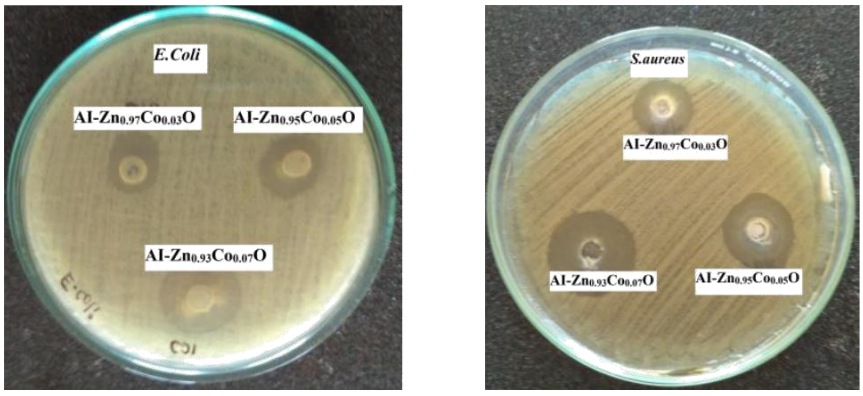

Figure 5: Antibacterial activity of AI gum stabilized Co doped ZnO nanoparticles against *Escherichia coli* and *Staphylococcus aureus*

3.4 Antifungal applications

The zone of inhibition of two fungal strains, *Aspergillus fumigatus* and *Candida albicans* are shown in Figure 6 and the values are given in Table 5. The maximum zone of inhibition was observed for AI-Zn0.93Co0.07O and less activity of AI-Zn0.95Co0.05O, AI-Zn0.97Co0.03O nanoparticles against fungus may be attributed to the complex cell wall structure of the fungus. The results explain ZnO nanoparticles which act against the water contamination, allergic reactions, and food poisoning and also act as drug resistant pneumonia. Hence, AI gum stabilized Co doped ZnO nanoparticles are used in pharmaceuticals to prepare best *anti-drug against pneumonia*.

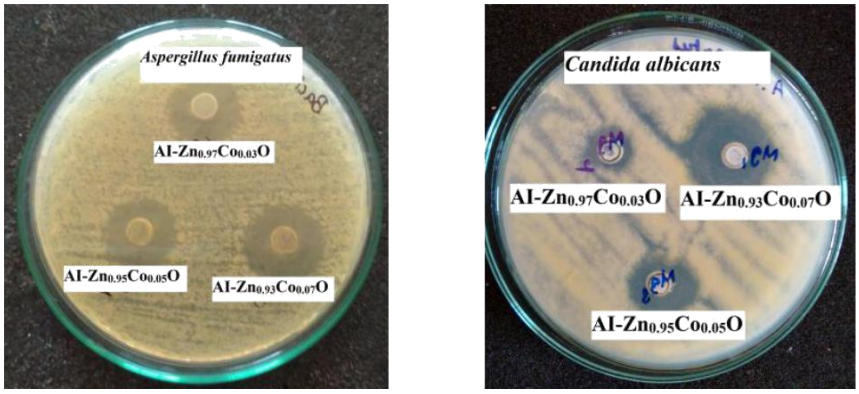

Figure 6: Antifungal activity of Co doped ZnO nanoparticles against *Aspergillus fumigatus* and *Candida albians*

Table 5: Antifungal assay of AI gum stabilized Co doped ZnO nanoparticles

S.No	Sample code	Zone of inhibition(mm)	
		Aspergillus fumigatus	***Candida albicans***
1	AI-Zn0.97 Co 0.03O	16	10
2	AI-Zn0.95 Co 0.05O	19	11
3	AI-Zn0.93 Co 0.07O	20	13

IV. Conclusion

In summary, AI gum stabilized Co doped ZnO hexagonal nanocrystalline (Zn1-xCoxO, where x = 0.03, 0.05, 0.07 g) were successfully synthesized using a simple wet chemical technique. Co dopant does not affect the crystalline structure and morphology of ZnO but the average particle size got increased, which is confirmed through XRD and FESEM results. The antimicrobial activity of the AI gum stabilized ZnO nanoparticles can be improved by Co doping

References

[1]. F. Yakuphanoglu, Reliab. 51 (2011) 2195–2199
[2]. C.F. Wang, B. Hu, H.H. Yi, Optik Y. Liu, Y. Li, H. Zheng, J. Nanomater. 20139.
[3]. S.K. Arya, S. Saha, J.E.R. Vick, V. Gupta, S. Bhansali, S.P. Singh Anal. Chim. Acta 737 (2012) 1–21
[4]. J. Xu, J. Han, Y. Zhang, Y. Sun, B. Xie, Sensors Actuators B. 132 (2008) 334–339
[5]. S. Wibowo, I. Nurhasanah, E. Hidayanto, H. Hadiyanto. Int. J. Chem. Eng. (2016) 20166
[6]. H. Sutanto, I. Nurhasanah, E. Hidayanto, Mater. Sci. Forum. 827 (2015) 3–6
[7]. M. Yan, H.T. Zhang, E.J. Widjaja, R.P.H. Chang, 94 (2003) 5240.
[8]. Huihu Wang, Seonghoon Baek, Jaejin Song, Jonghyuck Lee, Sangwoo Lim, Nanotechnology 19 (2008) 075607.

[9]. Chao Liu, Haiping He, Luwei Sun, Qian Yang, Zhizhen Ye, Lanlan Chen, J. Appl. Phys. 109 (2011) 053507.
[10]. K.W. Liu, M. Sakurai, M. Aono, J. Appl. Phys. 108 (2010) 043516.
[11]. Jahyun Yang, Juneyoung Lee, Kyungtaek Im, Sangwoo Lim, physica E 42 (2009) 51.
[12]. Z.F. Wu, X.M. Wu, L.J. Zhung, B. Hong, X.M. Yang, X.M. Chen, Q. Chen, Mater. Lett. 64 (2010) 472.
[13]. Te-Hua Fang, Shao-Hui Kang, J. Alloy. Compd. 492 (2010) 536.
[14]. Antonino Gulino, Ignazio Fragala, Chem. Mater. 14 (2002) 116.
[15]. G. Srinivasan, R.T. Rajendra Kumar, J.Kumar, Opt. Mater. 30 (2007) 314.
[16]. M.H. Mamat, Z. Khusaimi, M.F. Malek, M.Z. Musa, M. Rusop, AIP Conf. Proc. 1341 (2011) 440.
[17]. P. Koidl, Phys. Rev. B 15 (1977) 2493-2499.
[18]. C.A. Johnson, A. Cohn, T. Kaspar, S.A. Chambers, G.M. Salley, D.R. Gamelin, Phys. Rev. B 84 (2011) 125203.
[19]. B.D. Culity, S.R. Stock, Elements of X-ray Diffraction, Prentice Hall, New Jersey, 2001.
[20]. A. Sivagamasundari, R. Puaze, S. Chandrasekar, S. Rajagopan, R. Kannan, Appl. Nanosci. (2012) (13204-012-0146-0).
[21]. P.Stoimonve, R.K.Klinger, G.L.Marchin, K.J.Klabunde, Langmuir, 18(2002)6679-6686.
[22]. Mohammad Mansoob Khan, Sajid Ali Ansari, Mohammad Ehtisham Khan, Mohd Omaish Ansari, Bong-Ki Min & Moo Hwan Cho, New Journal of Chemistry. 39 (2015) 2758-2766.
[23]. S.Snega, K.Ravichandran, M. Baneto, Journal of material science and technology, 31(2015)759-765.